Desalination and Water Treatment
www.deswater.com

doi:10.5004/dwt.2017.0742

73 (2017) 64–72
April

Heat transfer prediction on flat solar collectors for the water purification system integrated to an absorption heat transformer

T. Hernández[a], S.G. Pérez[a], O. Flores[a], J.A. Hernández[b,*], D. Juárez-Romero[b], A. Álvarez[b], A. Huicochea[b], J.V. Galaviz-Rodriguez[c]

[a]*Posgrado en Ingeniería y Ciencias Aplicadas de la Universidad Autónoma del Estado de Morelos, Av. Universidad No. 1001, Col Chamilpa, CP. 62209, Cuernavaca, Morelos, México, Tel. +52 01 777 3297084; emails: teresa.hernandez@alumnos.uaem.mx (T. Hernández), sandro.perez@uaem.mx (S.G. Pérez), oliver.flores@uaem.mx (O. Flores)*
[b]*Centro de Investigación en Ingeniería y Ciencias Aplicadas (CIICAp), Universidad Autónoma del Estado de Morelos (UAEM), Av. Universidad No. 1001, Col Chamilpa, CP. 62209, Cuernavaca, Morelos, México, Tel. +52 01 777 3297084; emails: alfredo@uaem.mx (J.A. Hernández), djuarez@uaem.mx (D. Juárez-Romero), aalvarez@uaem.mx (A. Álvarez), huico_chea@uaem.mx (A. Huicochea)*
[c]*Carretera al Carmen Xalpatlahuaya SN, Carmen Xalpatlahuaya, 90500 Huamantla, Tlax, email: galaviz_4@hotmail.com (J.V. Galaviz-Rodriguez)*

Received 29 June 2016; Accepted 20 September 2016

ABSTRACT

This paper analyzes the prediction of the heat transformer obtained by two flat solar collectors' systems configured in series and parallel, as well as a third system which occurs with the union of the two previous. Solar flat collectors' systems were coupled to water heating energy source directed to integrated absorption heat transformer to a water purification system, maximizing efficiency. A feed-forward ANN (Artificial neural network) with standard BP (back propagation) algorithm was applied to heat transformer prediction. In view of statistical performance criteria i.e., RMSE (root mean square error) and R^2 (correlation coefficient), a supervised ANN with 5-5-1 topology (five inputs, five neurons in the hidden layer and one output layer) and *Levenberg–Marquardt* training algorithm represented the optimal model. This ANN considers useful total irradiation, water temperature in the heating tank, sampling time (second, day and month) as input parameters; and the heat gained by the water in the tank of warming as output parameter. The numerical results for the simulations of the heat output gained, for these 38 tests on each configuration, had an $R^2_{\text{series}} \geq 0.994$, $R^2_{\text{parallel}} \geq 0.998$, $R^2_{\text{coupled}} \geq 0.994$ with regard to experimental results. The proposed ANN models were appropriated to control the system.

Keywords: Artificial neural network; Solar energy; Absorption heat transformer

1. Introduction

Solar energy is the most important renewable source on earth; however, only a little amount is advantageous used. The high level of solar radiation coming to our planet can be used to develop new alternatives on production of power free of atmospheric pollutants. In lots of applications regarding solar technologies, flat solar collectors have been of great interest; they are capable mechanisms to turn solar radiation into useful heat for different procedures where a green energy source is required, reaching temperatures of 82°C.

The running water vital for human life is dropping as human population increases worldwide, this issue

*Corresponding author.

Presented at the EDS conference on Desalination for the Environment: Clean Water and Energy, Rome, Italy, 22–26 May 2016.

endeavors to look for alternatives to face this challenge. The thermal transformers have proved to be an efficient technology to purify the fluids at low cost. They work with heat coming from renewable energy without affecting the environment [1].

In this task, the thermal transformer was tied to a system with seven solar flat collectors interconnected in a parallel row, in order to take advantage of solar power to activate the thermodynamic cycle. Fig. 1 shows the system of solar heating connected to the thermal transformer.

The reported results on the examination of solar collectors, confirm their use as a source of energy to the thermal transformer to activate the thermodynamic cycle. Ayompe and Duffy [2] analyzed the thermal behavior during 1 year, over a system of flat solar collectors in Dublin, Ireland. The maximum temperature recorded at the exit was 70.4°C, while the maximum temperature of water inside the deposit was 59.9°C and the average daily energy collected in a year was 19.6 MJ/d.

The increase of the efficiency in thermal transformers through the embedding of solar collectors has been only limited researched. Sözen et al. [3], developed a prototype system of parabolic solar power integrated in a thermal transformer through absorption, using as an achievement blend water-ammoniac (AHP), the collected heat was used as a source of energy to the generator, reaching the required temperature needed of 60°C. Chen et al. [4] developed a theoretical-experimental work in a heating system made up by solar collectors connected in a series and connected to a thermal transformer (SAGCHP), installed in the Academy of Sciences in Shijiazhuang. The authors [4] obtained from the system (SAGCHP) a high thermal efficiency; 4,200 W of solar heating power obtained by the solar collector system and 95% of the energy is used to start the cycle of heat transformer in the evaporator, proposing the use of solar irradiance captured as an energy source for the heat transformer.

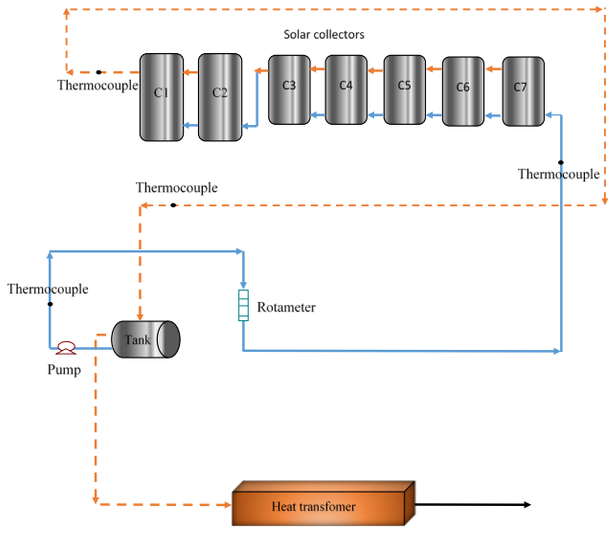

Fig. 1. System of solar heating connected to the thermal transformer.

The modeling and simulation are tools used to evaluate equipment, allowing to obtain the behavior of a design given without the need to test the physical device. Hussein et al. [5] worked on a theoretical-experimental work on a solar collector of flat plate. The ruling equations of the system were solved through the technology of finite differences, obtaining a discrepancy in the thermal efficiency from 5.3% to 8.9%, in a schedule from 9 am to 5:30 pm. Hamdy et al. [6] accomplished a work to determine the optimal inclination of a solar collector by using three mathematical models [7–9]. The authors [6] reached better results with the model [8]. This model takes into account three important factors: (1) geometrical representation of the sky dome, (2) the conditions of solar irradiation and (3) a statistical parameter relating the above two factors. The best results of the model were as follows: RMSE = 1.16% and R^2 = 1. From the results it is concluded that the optimum tilt depends on the season; during the winter months the best tilt for maximum irradiance is 43.33° south, while in summer days maximum radiation is obtained with an almost horizontal tilt.

Powerful tools that can be used in the mathematical interpretation of solar thermal systems are the artificial neural networks (ANN) [10]. The neuronal networks are an excellent alternative for the dynamic modeling; they are based on stochastic models which allow solving mathematically a complex issue; the system is interpreted as a flight recorder and the obtained model will be a role from the behavior of the variables of entrance and exit from the component in trial.

Wei et al. [11] studied the effect of $CaCl_2$ solution at different concentrations (3%, 9%, 15%, 21%, and 27%) and a source of energy in the COP of a heat pump using an ANN. Correlation coefficient, mean relative error and root mean squared error values were calculated. The results showed that the discrepancy in values *R*, MRE, RMSE between the training of the ANN and those experimental values for the COP was good: 0.995 (0.996), 2.09% (1.89%), and 0.005 (0.060), respectively. Amiri et al. [12] developed an ANN to model and predict the phenomenon of natural convection in two arrays of cylinders; Vertical and inclined. The discrepancy between experimental and predicted values by the ANN is very small, which means that the ANN model proposed has high precision and can be used to simulate experiments. Fernández et al. [13] performed an ANN to estimate the maximum power of a low concentration photovoltaic module. The model takes into account the following parameters: direct irradiation, diffuse irradiation, module temperature, angle of incidence transverse and longitudinal. The results show that the model can be proposed to estimate the maximum power of a photovoltaic module low concentration; R^2 = 0.99, MBE = 0.05%, RMSE = 2.32%. Morales et al. [14] conducted a model through the use of an ANN to predict the COP of a heat transformer by absorption. The architecture of the ANN consisted of 16 neurons in the input layer, seven neurons in the hidden layer and one neuron in the output layer. The results of the neuronal model showed a good relationship with the experimental data and retrieved a coefficient of correlation near one and a value of RMSE = 0.0052.

This report is focused in the use of an ANN to forecast the collected heat in a system of flat solar collectors

embedded to a thermal transformer. As the main contribution of this paper is to propose a source of clean energy (flat solar collector system configured in series and parallel as well as a third which occurs with the union of the two previous) to start the cycle heat transformer; consequently, the objective of this work is to developed an ANN for the prediction of heat transfer in the coupled system which consist in seven flat solar collectors connected to absorption heat transformer integrated at the water purification system.

2. Materials and methods

The system of solar heating is made up of seven flat collectors inclined 17.86° to the south. Each one has a glass insulating cover on the front side, an absorbing plate of solar radiation with nine blades of dark color copper, a system of piping out of copper to the rear side of the absorbing plate and a steel box with polyurethane isolation. Fig. 2 shows the system of flat solar collector. Table 1 describes the configuration and dimensions of the flat solar collectors.

The water runs through the copper piping which is in contact with the absorbing plate of solar radiation, and is sent through a pump to a storage tank made out of carbon steel, isolated with a polyurethane cover of 1 ½". The measures of the tank are: height 1.80 m, diameter 0.68 m, capacity 500 L. Fig. 3 shows the storage tank connected to the flat solar collector system. Fig. 4 shows the schematic diagram of the solar heating system used as an energy source for a thermal transformer, integrated to a system of cleansing water.

The test consisted in checking three systems of flat solar collectors; series, parallel, and a third one, which occurs by gathering the first two (coupled). The system of flat solar collector was tested during 9 months (January–September) from 8 a.m.–5 p.m. To measure the heating fluids supplied to the generator, a fluxometer was used with a maximum flux of measurement of 15 L/min, with accuracy of ± 3% in the measurement of the whole ratio. For the temperature measure in the system of flat solar collector thermo pairs type T, a thermometer of reference (± 0.1°C) was used resulting in an uncertainty of ± 0.2°C for each thermo pair. A data acquirer was used from the Agilent Technologies brand, series 34970A with 20 channels of voltage access for the direct measurement of voltage from the thermo pairs. To measure the solar radiation a pyranometer was used with a spectrum range of –300 nm to 2.5 μm with an accuracy of 1% in the measurement of the total scale.

The heat transfer gained $\dot{Q}_{cltd}$ in the water deposit was worked out with the difference of temperatures to the inlet (T_{in}) and outlet (T_{out}) of the fluid in contact with the absorbing plate of solar radiation, the mass flow $\dot{Q}$ and heat capacity (Cp), according to the Eq. (1):

$$\dot{Q}_{cltd} = \dot{m}Cp\left(T_{in} - T_{out}\right) \quad (1)$$

Table 2 shows the profits of the heat transfer for the conditions of operation obtained for 9 months for each system of flat solar collector, enough data base to develop the artificial neuronal network.

Fig. 2. Flat solar collector system.

Table 1
Dimensions of the flat solar collector system

Configuration	Collector	Length (m)	Width (m)	Total area (m^2)
Series	C1	2.05	0.93	13.98
	C2	2.05	0.93	
Parallel	C3	1.85	1.10	
	C4	1.85	1.10	
	C5	1.85	1.10	
	C6	1.85	1.10	
	C7	1.85	1.10	

Fig. 3. Storage tank.

3. Artificial neuronal network

The recommended methodology to forecast the heat transfer in the system of flat solar collector is ANN, which is a nonlinear mapping system, with a structure based on principles observed in the nerve system of humans and animals. Fig. 5 shows an artificial neuron, which tries to model after the behavior of the biological neuron. The body of the

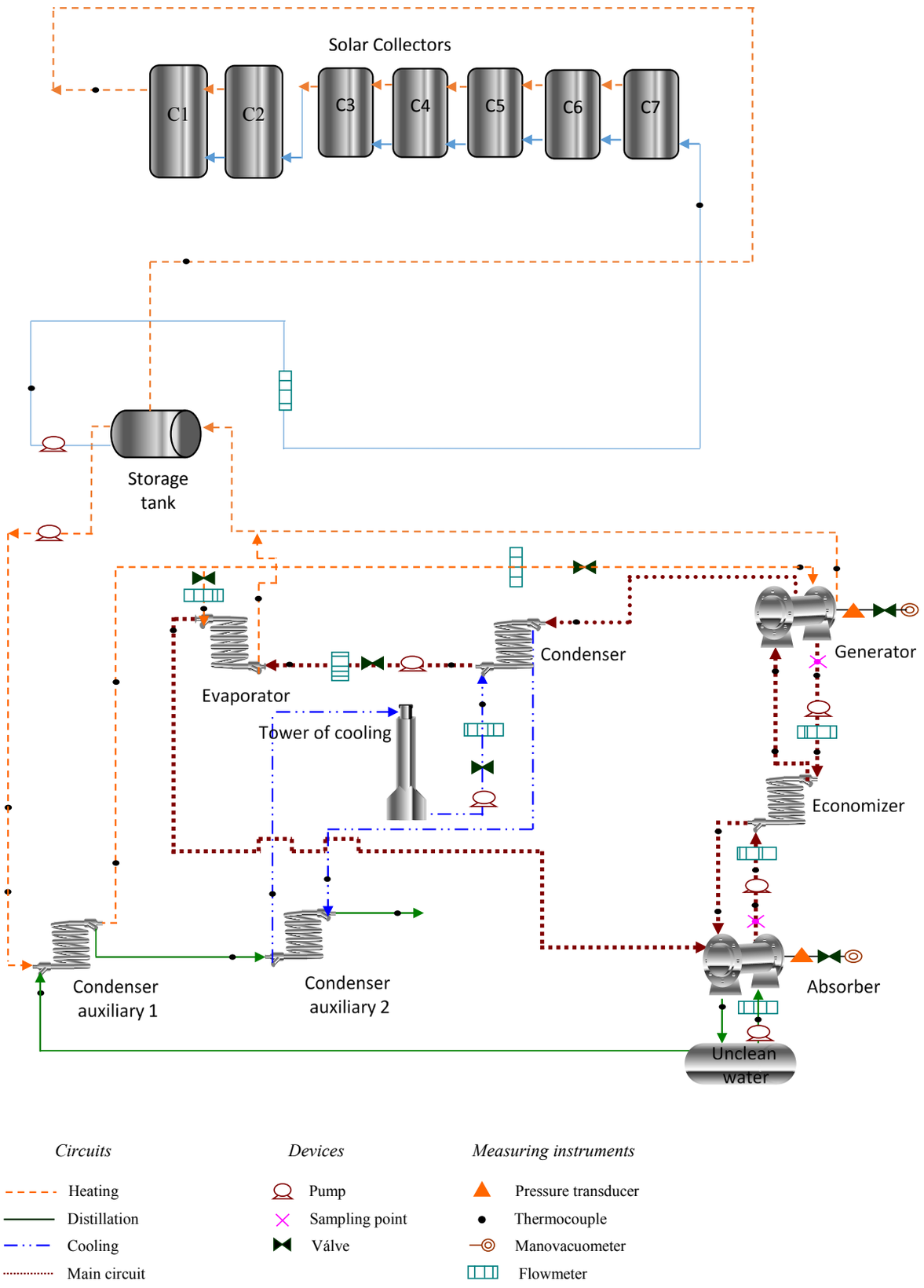

Fig. 4. Diagram schematic detailed of the system collector solar attached to the heat transformer.

Table 2
Heat collected in the different operating conditions

Month	Day	Hour	Irradiation W/m²	Serie			Paralelo			Acoplado		
				T_{in} [°C]	T_{out} [°C]	$\dot{Q}_{cltd}$ [W]	T_{in} [°C]	T_{out} [°C]	$\dot{Q}_{cltd}$ [W]	T_{in} [°C]	T_{out} [°C]	$\dot{Q}_{cltd}$ [W]
1	4		663–787	29.40–66.08	32.10–66.80	653–2,449	25.70–64.10	29.40–66.08	1,796–4,081	25.70–64.10	32.70–66.80	2,449–6,349
	14		684–814	27.20–63.10	29.60–64.20	997–2,394	22.80–59.90	27.20–63.10	2,685–3,991	22.80–59.90	29.60–64.20	3,900–6,168
2	13		617–897	43.50–77.09	48.80–78.10	825–4,807	43.50–72.70	46.01–77.09	934–6,077	43.50–72.70	48.80–75.50	2,539–8,163
	15		771–870	46.10–75.25	48.80–76.10	997–2,812	40.03–73.10	46.20–75.80	272–7,166	40.02–73.10	48.80–76.10	2,449–9,978
	19		786–879	48.60–72.04	50.04–73.80	362–1,814	39.40–71.10	48.60–72.04	786–879	39.40–71.10	50.03–73.80	2,449–11,429
3	9		739–881	34.30–75.10	35.70–76.20	725–1,759	31.10–70.09	34.30–75.10	2,095–5,261	31.10–70.04	35.70–76.20	3,447–5,986
	23		842–1,046	30.36–80.86	32.40–82.20	970–1,850	29.01–78.03	30.36–80.86	1,233–9,370	29.04–78.05	32.40–82.20	3,084–10,794
	30		895–977	31.40–75.03	33.70–76.60	272–3,320	29.30–71.80	31.40–75.02	1,904–5,351	29.30–71.80	33.70–76.60	2,539–7,982
4	5		932–975	34.50–75.30	35.70–76.20	725–2,167	33.03–72.02	34.50–75.30	1,279–6,077	33.02–72.05	35.70–76.20	2,449–6,803
	12		739–1,037	34.90–80.15	36.06–81.90	997–2,186	30.50–66.78	34.90–80.15	1,950–5,986	30.50–78.03	36.05–81.90	3,537–7,075
	16		925–1,027	36.08–82.07	36.90–82.10	27–2,358	31.20–81.80	36.02–82.07	244–6,077	31.20–81.80	36.90–82.10	272–7,891
	19		866–926	36.30–82.65	38.04–84.50	126–1,968	34.02–78.10	36.30–82.65	2,086–7,919	34.02–78.04	38.05–84.50	3,628–9,887
5	17		904–932	49.28–68.72	51.58–69.89	1,061–5,841	43.03–63.86	49.61–68.72	1,868–5,968	43.03–63.86	51.58–78.25	5,243–13,053
	18		906–936	49.90–83.09	55.38–85.33	2,031–7,701	47.12–71.21	49.90–83.09	2,521–10,776	47.12–71.21	55.38–85.33	7,492–12,808
	19		905–949	54.67–73.34	55.95–83.56	1,161–9,270	50.58–69.64	54.67–73.34	3,356–6,903	50.58–69.64	55.95–83.56	4,871–12,626
	29		906–953	53.98–80.87	55.66–84.44	1,523–13,842	48.85–70.42	53.98–80.87	1,741–9,769	48.85–70.42	55.66–84.44	6,177–12,717
6	11		764–1,088	44.51–62.36	44.58–63.72	63–1,932	44.32–60.50	44.51–62.36	172–2,567	44.32–60.50	44.58–63.72	235–4,499
	12	8–17	661–1,075	44.54–63.27	44.70–66.76	145–6,322	44.39–52.61	44.54–63.27	136–10,885	44.39–52.61	44.70–66.76	281–14,051
	17		344–1,076	52.95–68.96	56.67–72.08	2,830–4,544	46.88–60.08	52.95–68.96	3,764–8,055	46.88–60.08	56.67–72.08	8,309–10,885
	19		568–892	55.16–71.43	56.02–74.22	780–5,088	54.59–61.16	55.16–71.43	517–9,315	54.49–61.16	56.02–74.22	1,297–11,846
	25		487–1,121	44.50–55.27	44.58–58.76	54–3,165	44.32–54.40	44.50–55.27	163–4,199	44.32–54.88	44.58–58.76	542–1,230
	26		611–1,067	47.56–69.93	49.03–75.07	126–4,662	47.56–66.27	47.80–69.93	217–6,467	47.80–66.27	49.03–75.07	526–11,130
7	4		807–1,047	47.07–59.35	47.80–63.55	725–7,030	44.10–53.95	47.03–59.35	54–10,613	44.10–53.95	47.80–63.55	7, 801–7,643
	8		669–943	34.26–45.51	36.52–44.97	63–2,050	32.49–43.48	34.26–45.51	698–1,841	32.49–43.48	36.52–44.97	589–3,655
	9		900–1,034	37.28–67.02	38.89–69.48	662–2,231	34.94–61.50	37.28–67.02	1,669–5,007	34.94–61.50	38.89–69.48	2,331–7,238
	10		972–1,100	45.23–67.02	45.65–69.48	36–2,231	44.29–56.70	45.23–63.99	535–6,612	44.29–56.70	45.65–69.76	1,233–11,846
	11		939–1,084	36.71–72.23	40.08–72.51	253–3,056	22.99–67.80	36.71–72.23	689–12,445	22.99–67.80	40.08–72.51	1,260–15,502
	12		707–901	38.96–50.73	41.73–54.44	335–3,365	35.64–45.14	38.96–50.73	45–6,104	35.64–45.14	41.73–54.44	335–9,470
8	3		115–1,127	50.04–73.15	51.55–78.65	653–5,079	49.09–69.02	50.04–73.15	671–6,113	49.30–69.02	51.55–78.65	2,040–11,193
	29		990–1,154	36.10–57.65	37.34–59.49	208–1,669	35.39–55.33	36.10–57.65	644–4,227	35.39–55.33	36.10–59.49	644–4,481
	30		850–1,061	45.77–77.01	47.80–83.50	1,179–5,896	43.99–71.42	45.77–77.04	725–5,061	43.99–71.42	47.80–83.50	1,904–10,957
	31		884–1,080	54.20–74.90	57.87–82.15	1,596–6,576	51.55–69.30	54.20–74.90	2,403–5,079	51.55–69.30	57.87–82.15	5,732–11,656
9	3		809–1,121	39.09–69.96	39.66–73.20	598–2,939	37.95–63.40	39.04–69.96	308–5,950	37.95–63.40	39.66–73.20	1,551–8,889
	9		995–1,196	40.47–66.29	45.30–74.40	4,381–7,356	38.92–60.32	40.47–66.29	1,406–7,302	38.92–60.32	45.30–74.40	5,787–12,772
	23		610–982	43.55–68.96	46.01–73.20	2,222–3,991	39.90–60.10	43.55–68.96	3,310–10,522	39.90–60.10	46.02–73.20	5,533–14,513

neuron is represented as a lineal increaser of external stimuli z_j, followed by a nonlinear function $y_j = f(z_j)$. The function $f(z_j)$ is called activation function, and it is the function that uses the addition of stimuli to determine the activity of the neuron exit. Fig. 5 is the base model of most of the architectures of ANN that are interconnected among themselves [15].

The ANN is a big number of simple processors linked by connections with weights.

The models of artificial neuronal networks have as a fundamental element, a structure with a net shape, made by neurons interconnected among them, representing the brain functional process which includes through its interaction along the time, the outcomes of other neurons. Each entrance (In_i), has a weight value assigned accordingly (W_i). The addition of the entrance weights and the bias (b), produces the entrance (n), to move later to a transfer function that will generate an exit according to Eq. (2)

$$n_s = W_{i\{s,1\}} In_1 + W_{i\{s,2\}} In_2 + \cdots + W_{i\{s,k\}} In_k + b_{1s} \quad (2)$$

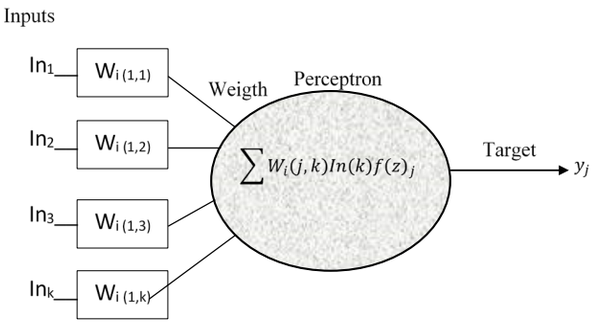

Fig. 5. Base model of ANN.

The values associated with the hidden cover, are associated to the matrix of connection of W_i y b_1. The output layer obtains the considered addition of signals provided by the hidden layer, and the associated coefficients are gathered in matrixes W_o y b_2. By using the matrix remark, the output of the network can be given by Eq. (3).

$$\text{Output}_l = g\left(W_0\left[f\left(W_i In_k + b1_s\right)\right] + b_2\right) \quad (3)$$

The function in the hidden cover f can be sigmoid, tangent hyperbolic, among others. In MATLAB® different functions exist for activating, as tansing, hardlim and purelin, among others, which enhances the approximations required to make, by employing ANN. In this work, a function of tangent hyperbolic transfer sigmoid (TANSIG) and a lineal transfer function (PURELIN) were used for f and g, respectively. Considering the transfer functions in Eqs. (3) and (4) is determined as follows:

$$\text{Output}_l = \text{PURELIN}\left\{W_0\left[\text{TANSIG}\left(W_i In_k + b_{1s}\right)\right] b_{2l}\right\} \quad (4)$$

The transfer functions f and g, are given by Eqs. (5) and (6), respectively.

$$\text{TANSIG} = f = \frac{2}{1+\exp(-2n_s)} - 1 \quad (5)$$

$$\text{PURELIN} = g = n_s \quad (6)$$

where s, is the number of neurons in the hidden layer, k is number of neurons in the cover of entrance, letter l is the number of neurons in the out layer, W_i, W_o are weights and b_1, b_2 bias, respectively. The learning process of the ANN was achieved through the adjustment of weights, in the connections among neurons. Fig. 6 shows the use of optimization algorithm *Levenberg–Marquardt* to reduce the discrepancy between the experimental results and the simulated results.

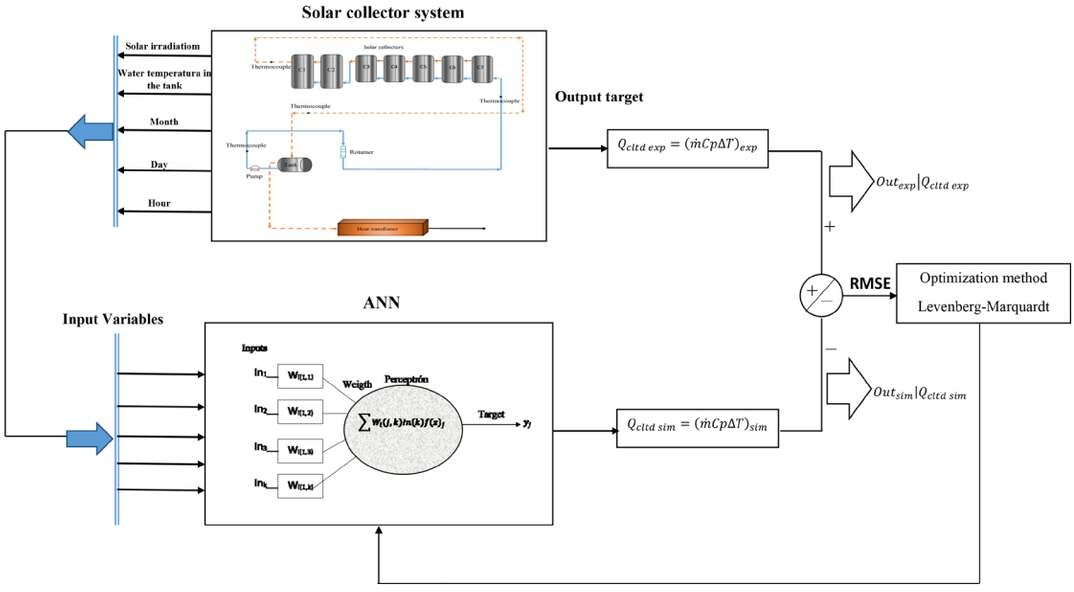

Fig. 6. Procedure used for the training of the network.

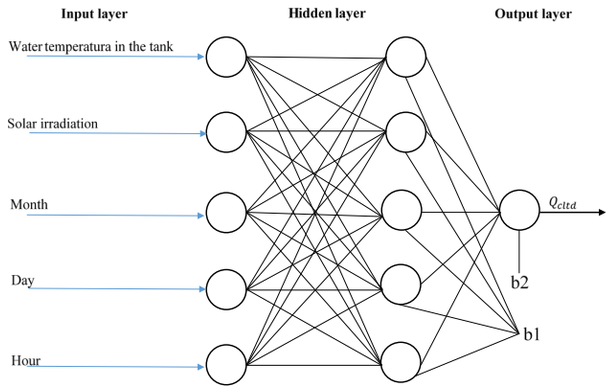

Fig. 7. Architecture of the ANN.

4. Neural model proposed in the flat solar collector system

Fig. 7 shows the neuronal model used to predict the behavior of the heat transfer obtained by the system of flat solar collector in its three configurations (series, parallel and coupled). It was found that architecture with five neurons in the hidden layer (30 weights and 6 bias) was enough to predict the heating gain in the storage tank. A similar research was done by Gomez et al. [16] in a horizontal plate of solar collector, considering the solar radiation and the time of sampling as entrance variables.

Table 3 shows the adjusted parameters (W_i, W_o, b_1 and b_2) of the neuronal network planned (five inputs, five neurons in the hidden layer and one output). These parameters are used in the ANN model to simulate the values of collected heating in the storage tank coupled in the system of flat solar collector configured in series, parallel and coupled.

Fig. 8 shows the values worked out on trial of collected heating in the storage tank of the system of flat solar collector, configured in series, parallel and coupled, regarding the simulated values. We can observe that the simulated values of collected heating are a good prediction of the experimenting values with a coefficient of determination; $R^2_{\text{series}} \geq 0.994$, $R^2_{\text{parallel}} \geq 0.998$, R^2_{coupled} 0.994, respectively; this proves the efficiency of the model to predict the values of collected heating and the importance of the artificial neuronal network in the simulation for the interpretation of behavior in the collected heating of systems of flat solar collectors.

Based on the previous architecture of the ANN (Fig. 7), the neuronal model can be represented with the following equation:

$$Q_{\text{cltd}} = \text{PURELIN}\left\{\left[\text{TANSIG}\left(W_i In_k + b_{1s}\right)\right] b_{2l}\right\} \tag{7}$$

Eq. (7) is not complex, it is based on simple Arithmetic, and it can be used in the application of the on-line estimation of industrial actions [17].

On the other hand weights calculated with the ANN in Table 3 they can be used to calculate the level of influence of each input variables concerning the modeling output. The Eq. (8) it has been proposed based on the partitioning of connection weights to obtain the importance of the input variables [18,19]. Eq. (8) was applied the coupled ANN model.

Table 3
Adjusted parameters (weight and bias) in the neuronal planned with $L = 1$, $S = 5$, K

Series					
$W_{i(S,K)}$	–7.6832	3.5705	–22.3439	–1.8610	1.9833
	1.7883	–2.0800	–9.8299	–3.6890	–0.9949
	1.9375	–7.0558	3.1268	1.6874	1.4488
	1.3386	–1.7440	12.0250	0.8764	3.7087
	0.0911	–0.6227	–1.7642	–0.0316	0.0177
$W_{0(L,S)}$	–8.8055	–0.0223	0.0186	0.0270	–0.7351
$b1_{(S,1)}$	26.8141				
	4.6511				
	–32.0348				
	–12.3759				
	2.8173				
$b2_{(L,1)}$	9.5950				
Parallel					
$W_{i(S,K)}$	2.0610	0.7410	2.2515	8.5803	–0.5603
	0.5421	–0.0823	–0.2166	–2.3714	–0.2782
	–0.4913	0.0788	–0.0913	2.1517	2.4361
	–0.3773	0.4414	11.9917	4.1031	0.1752
	1.4569	0.4712	–8.9555	–1.0264	–0.7887
$W_{0(L,S)}$	0.2011	–1.7683	–1.9155	0.0928	–3.7421
$b1_{(S,1)}$	–12.1226				
	–0.7374				
	–0.5026				
	–10.8886				
	10.4302				
$b2_{(L,1)}$	4.2659				
Coupled					
$W_{i(S,K)}$	4.9443	–8.8032	1.4802	2.1157	0.1832
	–2.3966	5.0432	–5.0463	–2.0095	0.1304
	–3.5498	2.3587	12.0390	–0.7088	0.2473
	–0.0159	0.0006	0.2829	0.0470	0.0168
	–2.3630	–2.9290	1.6978	7.1617	0.6469
$W_{0(L,S)}$	–3.8350	–3.0843	0.0718	2.7588	–0.3354
$b1_{(S,1)}$	–5.1728				
	6.3006				
	–8.9733				
	–0.8939				
	–5.9012				
$b2_{(L,1)}$	0.9102				

$$I_j = \frac{\sum_{m=1}^{m=Nh}\left(\left(W_{jm}^{ih} / \sum_{k=1}^{Ni}\left|W_{km}^{ih}\right|\right) * \left|W_{mn}^{ho}\right|\right)}{\sum_{k=1}^{k=Ni}\left\{\sum_{m=1}^{m=Nh}\left(\left|W_{km}^{ih}\right| / \sum_{k=1}^{Ni}\left|W_{km}^{ih}\right|\right) * W_{mn}^{ho}\right\}} \tag{8}$$

where I_j represents the relative importance of the jth input variable on the output variable, N_i and N_h refers to the number of inputs and neurons in the hidden layer, respectively; W_s are the weights, the superscripts *'i'*, *'h'*

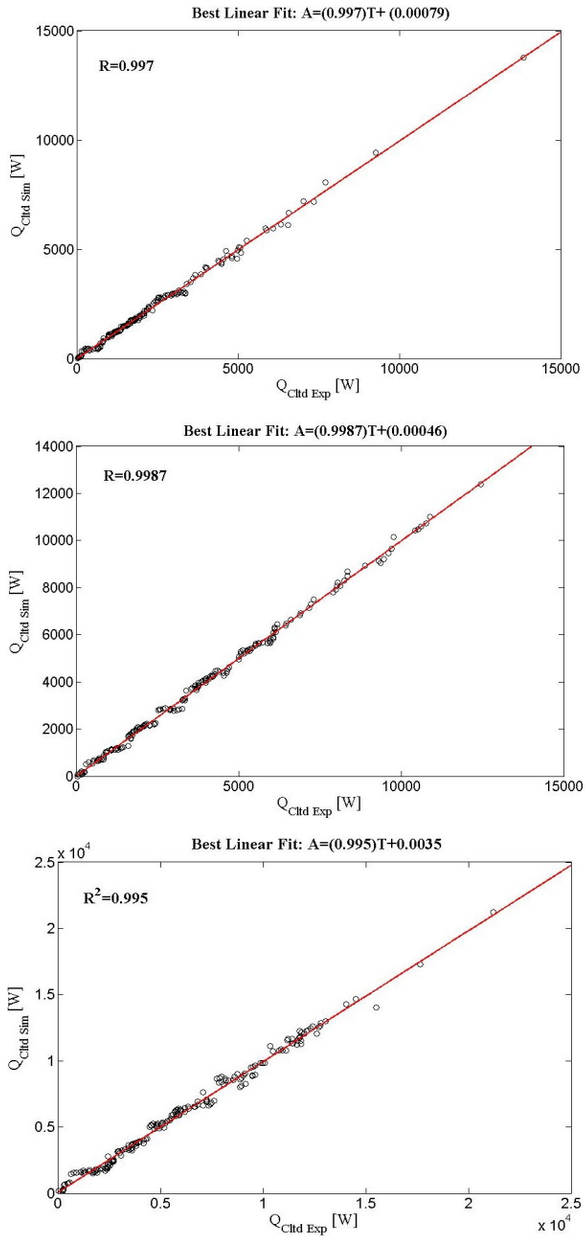

Fig. 8. Experimental collected heating vs. simulated collected heating.

and *'o'* refer to the layers (input, hidden and output) and the subscript *'k'*, *'m'* and *'n'* are neurons in layer input, hidden layer and output layer, respectively. The relative importance of the five input variables has been calculated according to Eq. (8) and shown in Fig. 9. As can be seen, most of the times except the variables have strong effects on the heat collected in the panels solar; it is for this reason that any of the variables can be neglected in this analysis. However, as expected, the solar irradiation and the month are most influential parameter in the process of heat collected in solar panels.

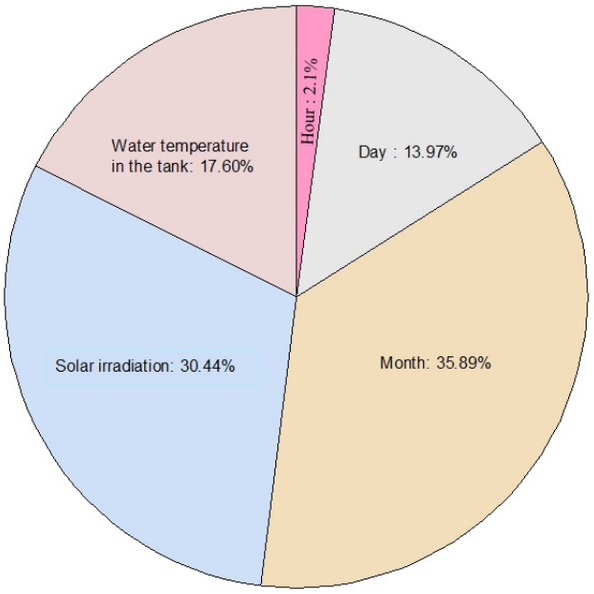

Fig. 9. Relative importance (%) of input variables on the value of collected heating.

5. Conclusions

This paper offers the application of ANN with the following topology: five neurons in the input layer, three neurons in the hidden layer, one neuron in the output layer and algorithm for training *Levenberg–Marquardt*. The parameter in the output layer is the collected heating in the storage tank of three systems of flat solar collectors configured in series, parallel, and a third one, which occurs with the gathering of the previous two, respectively. The neuronal model based on simple mathematical operations predicts the behavior of the heat collected with an error lower than 0.01%. The discrepancy between the experimental and simulated results, proposes ANN as a good tool to predict the heat collected in a flat solar collector system. At the same time it is concluded from experimental results of outlet temperature and collected heat (T_{minimun} = 30°C, T_{maximun} = 85°C, $\dot{Q}_{\text{cltd minimun}} = 54\,W$, $\dot{Q}_{\text{cltd maximum}} = 21230\,W$) that the flat solar collector system is a good source of energy to start the thermodynamic cycle of heat transformer. In addition, a study of the relevance of each of the input variables was done, based on the weights obtained by the ANN, allows visualizing the relative importance of the input variables in the heat collected.

References

[1] S. Smolen, M. Budnik-Rodz, Low rate energy use for heating and in industrial energy supply systems—some technical and economical aspects, Energy, 31 (2006) 2588–2603.
[2] L. Ayompe, A. Duffy, Analysis of the thermal performance of a solar water heating system with flat plate collectors in a temperate climate, Appl. Therm. Eng., 58 (2013) 447–454.
[3] A. Sözen, D. Altıparmak, H. Usta, Development and testing of a prototype of absorption heat pump system operated by solar energy, Appl. Therm. Eng., 22 (2002) 1847–1859.

[4] C. Xi, Y. Hongxing, L. Lin, W. Jinggang, L. Wei, Experimental studies on a ground coupled heat pump with solar thermal collectors for space heating, Energy, 36 (2011) 5292–5300.
[5] H. Hussein, M. Mohamad, A. El-Asfouri, Optimization of a wickless heat pipe flat plate solar collector, Energy Convers. Manage., 40 (1999) 1949–1961.
[6] H.K. Elminir, A.E. Ghitas, F. El-Hussainy, R. Hamid, M. Beheary, K.M. Abdel-Moneim, optimum solar flat-plate collector slope: case study for Helwan, Egypt, Energy Convers. Manage., 47 (2006) 624–637.
[7] R.C. Temps, K. Coulson, Solar radiation incident upon slopes of different orientations, Sol. Energy, 19 (1977) 179–184.
[8] R. Perez, R. Seals, P. Ineichen, R. Stewart, D. Menicucci, A new simplified version of the perez diffuse irradiance model for tilted surfaces, Sol. Energy, 39 (1987) 221–231.
[9] J. Bugler, The determination of hourly insolation on an inclined plane using a diffuse irradiance model based on hourly measured global horizontal insolation, Sol. Energy, 19 (1977) 477–491.
[10] H. Benli, Determination of thermal performance calculation of two different types solar air collectors with the use of artificial neural networks, Int. J. Heat Mass. Trans., 60 (2013) 1–7.
[11] X. Wei, N. Li, J. Peng, J. Cheng, L. Su, J. Hu, Analysis of the effect of the $CaCl_2$ mass fraction on the efficiency of a heat pump integrated heat-source tower using an artificial neural network model, Sustainability, 8 (2016) 1–14.
[12] A. Amiri, A. Karami, T. Yousefi, M. Zanjani, Artificial neural network to predict the natural convection from vertical and inclined arrays of horizontal cylinders, Pol. J. Chem. Tech., 14 (2012) 46–52.
[13] F. Fernández, F. Almonacid, N. Sarmah, P. Rodrigo, T. Mallick, P. Perez, A model based on artificial neuronal network for the prediction of the maximum power of a low concentration photovoltaic module for building integration, Sol. Energy, 100 (2014) 148–158.
[14] L.I. Morales, R.A. Conde-Gutiérrez, J.A. Hernández, A. Huicochea, D. Juarez-Romero, J. Siqueiros, Optimization of an absorption heat transformer with two-duplex components using inverse neural network and solved by genetic algorithm, Appl. Therm. Eng., 85 (2015) 322–333.
[15] P. Ponce, Artificial Intelligence Applications Engineering, First Ed., Alfaomega, 2010.
[16] J. Díaz-Gómez, A. Parrales, A. Álvarez, S. Silva-Martínez, D. Colorado, J. Hernández, Prediction of global solar radiation by artificial neural network based on a meteorological environmental data, Desal. Wat. Treat., 55 (2015) 3210–3217.
[17] A. Bassam, E. Santoyo, J. Andaverde, J. Hernández, O. Espinoza-Ojeda, Estimation of static formation temperatures in geothermal wells by using an artificial neural network approach, Comput. Geosci., 36 (2010) 1191–1199.
[18] A. Aleboyeh, M. Kasiri, M. Olya, H. Aleboyeh, Prediction of azo dye decolorization by uv/h 2 o 2 using artificial neural networks, Dyes Pigments, 77 (2008) 288–294.
[19] M. Kasiri, H. Aleboyeh, A. Aleboyeh, Modeling and optimization of heterogeneous photofenton process with response surface methodology and artificial neural networks, Environ. Sci. Technol., 42 (2008) 7970–7975.